

Superstructure formation and faceting in the Cu(210)-O system studied by scanning tunneling microscopy

A. T. S. Wee*

Department of Physics, National University of Singapore, Kent Ridge, Singapore 119260

J. S. Foord and R. G. Egdell

New Chemistry Laboratory, University of Oxford, South Parks Road, Oxford OX1 3QT, United Kingdom

J. B. Pethica

Department of Materials, University of Oxford, Parks Road, Oxford OX1 3PH, United Kingdom

(Received 17 June 1998)

The interaction of O on Cu(210) has been investigated by scanning tunneling microscopy. Adsorption at room temperature followed by high-temperature annealing leads to a series of mesoscopic superstructures ordered on different length scales ranging between 15 and 150 Å. By contrast, adsorption at high temperatures leads to the formation of a (2×1) superstructure similar to that found on Cu(110). [S0163-1829(98)50136-1]

Over the past few years, the scanning tunneling microscopy (STM) technique has been instrumental in establishing a consensus regarding the structure of O chemisorption reconstructions on low-index Cu surfaces.¹ O chemisorption on both Cu(110) and (100) surfaces leads to substantial reconstruction of the topmost Cu atom layer. Both reconstructions appear to receive stability from being able to accommodate O-Cu-O building blocks, of the sort needed to construct bulk Cu₂O.² Each O atom achieves a four-coordinate status with reasonable O-Cu bond lengths of 1.90 ± 0.01 Å. For Cu(110) in particular, the (2×1)-O phase is an “added row” structure with every other [001] Cu atom row absent, and O atoms occupy near collinear long-bridge sites in the added rows forming O-Cu-O chains.³⁻⁵

For higher-index Cu surfaces, scanning tunneling microscopy (STM) has been used to study oxygen-induced faceting on a nominally (610) oriented face of Cu at large oxygen exposures (>1000 L).⁶ On the Cu(210)-O system, an early LEED/AES study reported a clean (1×1) unreconstructed surface as well as (2×1) and (3×1) LEED patterns under certain conditions of oxygen exposure and heating.⁷ Fcc Cu{210} planes have a primitive unit cell which is oblique, with parameters $a=0.441$ nm, $b=0.361$ nm, and $\theta=114.1^\circ$. The (210) surface may be regarded as having the maximum step density in the [001] zone comprising {100} terraces two atom rows wide separated by monatomic {110} steps. It therefore occupies a pivotal position between the low index (100) and (110) planes and the higher index (n 10) planes which contain wider terraces. This paper reports the formation of superstructures and facets induced by room temperature (RT) O chemisorption on Cu(210) followed by high-temperature annealing. We show that the open Cu(210) surface restructures more easily than low-index Cu surfaces. A (2×1)-O added row structure can also form, but only during O adsorption at high temperatures.

The STM experiments were conducted in a ultrahigh vacuum (UHV) system incorporating a Omicron STM stage operated at room temperature (RT) as described in detail elsewhere.⁸ Electrochemically etched tungsten tips were used

throughout. The polished Cu(210) crystal was cleaned by repeated cycles of Ar⁺ sputtering (1.5 keV, 30 min) and annealing (900 K, 30 min) until good (1×1) LEED patterns were observed. STM images of clean Cu(210) show large (1×1) terraces separated by monatomic steps that showed evidence for dynamic fluctuations at RT, similar to that observed on clean Cu(110).⁹ Details of the clean Cu(210) surface are reported elsewhere.¹⁰ In these experiments, oxygen was introduced into the UHV chamber via a precision leak valve, and the pressure measured by an uncalibrated ion gauge. Oxygen exposures are reported in Langmuirs ($1 \text{ L} = 1 \times 10^{-6} \text{ Torr s}$).

Exposure of clean Cu(210) to oxygen at RT results in the roughening and pinning of step edges, formation of irregularly shaped troughs on terraces, and the appearance of islands with an approximately rectangular shape. Figure 1 shows a 300×300 Å² STM image after RT exposure to 61-L oxygen. The surface has roughened significantly and rectangular arrays of islands are formed with their long edges along the [001] direction. The interconnected island arrays are approximately 25–30-Å wide, comprising 6–8 Cu atom rows. As with previous RT STM studies of O on Cu, only the Cu atoms are imaged and not the O adatoms.³⁻⁵ We believe however that Cu-O rows oriented along the [001] direction are responsible for the preferential [001] orientation of the islands. The long edges of the islands show missing atoms with a periodicity of two or three times the Cu-Cu distance along the [001] direction (3.61 Å), consistent with additional half and one-third order streaks observed in LEED.

Annealing to 500–620 K after RT oxygen exposures between 1–500 L always resulted in superstructure formation as shown in Fig. 2(a). The image shows long-range spatial self-organization of the rectangular islands into a striped periodic structure with mesoscopic ordering along the [120] direction. Following Kern *et al.*¹¹ for O-Cu(110), we refer to this as a “supergrating.” The stripes run along the [001] direction with a grating periodicity of 28–30 Å or 6–7 Cu-O rows with a missing row between the stripes, presumably due to long-range repulsion. Larger STM scans show that the

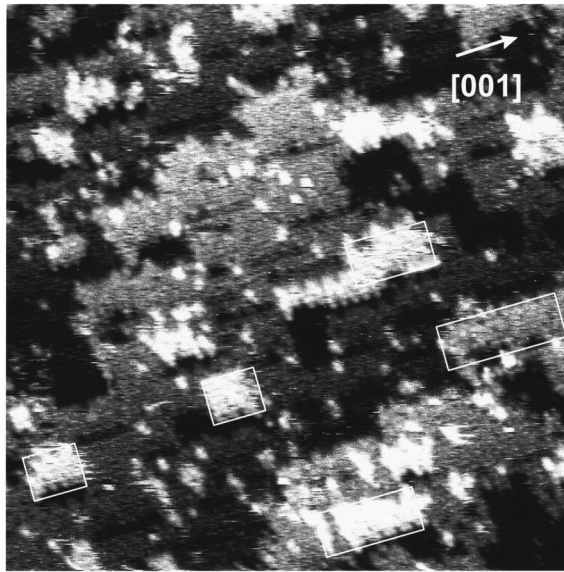


FIG. 1. $300 \times 300 \text{ \AA}^2$ STM image ($V_B = -1.0 \text{ V}$, $I_T = 0.25 \text{ nA}$) after RT oxygen exposure of clean Cu(210) to 61 L. Several rectangular islands are highlighted.

striped supergrating extends practically undisturbed across monatomic steps along the $[121]$ and $[1\bar{2}1]$ directions. Figure 2(a) also shows that up to three or four layers of these stripes could stack themselves on the stripes below, laterally displaced by less than one Cu-O row. Unlike the Cu(110)- (2×1) O supergrating which has a variable periodicity of between 60–140 Å depending on oxygen coverage and substrate temperature, the O-Cu(210) supergrating has a fixed periodicity in the oxygen exposure range used of 1–500 L. If we assume the Cu(210) supergrating also comprises Cu-O rows along the $[001]$ direction, the reduced spacing of 4.03 Å between the $[001]$ Cu-O rows compared to 5.12 Å for Cu(110)- (2×1) O could account for the narrower stripes observed (28–30 Å) due to larger repulsive forces.

Annealing of these periodic supergratings *in vacuo* for longer periods and at higher temperatures yielded a fascinating range of faceting behavior. This is in spite of the fact that some surface oxygen might be lost during annealing. Figure 2(b) shows a $300 \times 300 \text{ \AA}^2$ image after 70-L oxygen exposure at RT and subsequent annealing overnight at 680 K. The 30-Å period supergrating transforms into a series of 150-Å period ridges running along the $[001]$ direction. Corrugation profiles along the $[1\bar{2}0]$ direction reveal that these have a symmetrical sawtooth cross section, built up from a series of closely spaced terraces. Careful inspection of this atomically resolved image shows that the stepped planes generally comprise a three-atom-wide (210) terrace and a monatomic (100) step, i.e., in the generally accepted notation (S) - $[3(210) \times (100)]$. Figure 2(b) also shows a rectangular 30-Å stripe (highlighted by a box), wedged between two of these ridges, which has been partially transformed by the build up of Cu layers and the broadening of its base. Smaller area STM scans reveal that the Cu layers are not in registry, and that the Cu atom sits in approximately the three-fold hollow site. This would be expected for the growth of bulk Cu. The next question which needs to be addressed is the location of the O adatoms and their role in faceting and binding the new structures. There is no doubt that O is present since the corruga-

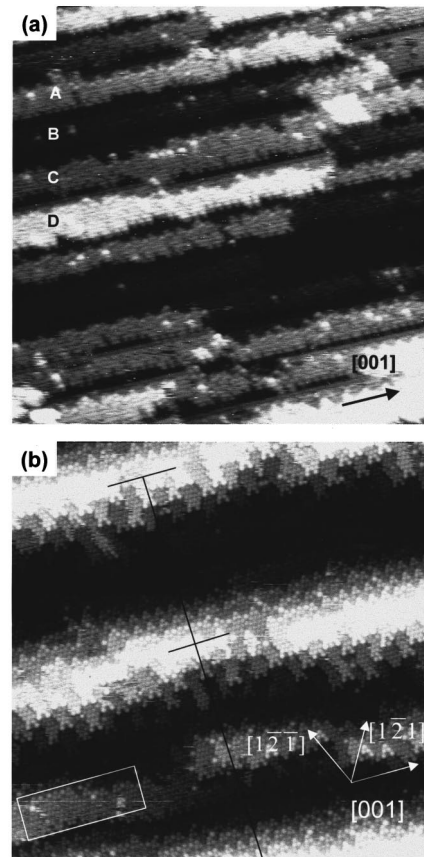


FIG. 2. (a) $300 \times 300 \text{ \AA}^2$ ($V_B = -1.0 \text{ V}$, $I_T = 0.30 \text{ nA}$) image after 500-L RT oxygen exposure and subsequent annealing to 620 K for a few minutes. Analysis of corrugation profiles shows that A and C are at the same height, whereas B is one unit cell below and D one above. (b) $300 \times 300 \text{ \AA}^2$ ($V_B = -50 \text{ mV}$, $I_T = 0.2 \text{ nA}$) image after surface in (a) was further annealed at 680 K overnight.

tion is much stronger than that of clean Cu: we find a corrugation of 0.3–0.4 Å along $[001]$ compared to 0.1–0.2 Å for the clean surface. Quantitative LEED studies will be required to deduce the O adatom positions in these reconstructions.

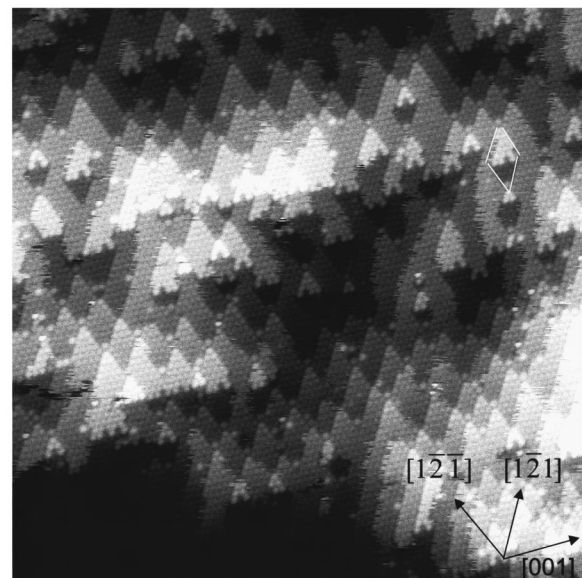


FIG. 3. $300 \times 300 \text{ \AA}^2$ image ($V_B = -0.2 \text{ V}$, $I_T = 1.0 \text{ nA}$) after surface in Fig. 2 was further annealed at 740 K overnight.

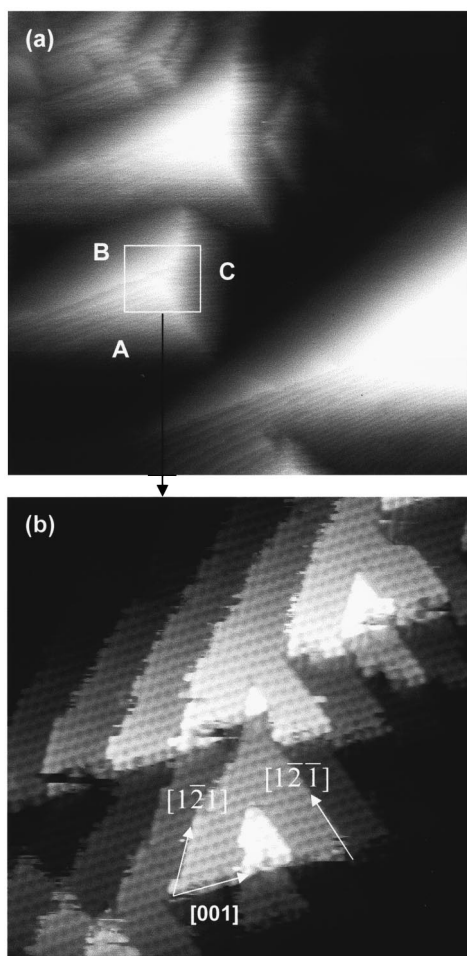


FIG. 4. (a) $2000 \times 2000 \text{ \AA}^2$ image ($V_B = -0.3 \text{ V}$, $I_T = 0.6 \text{ nA}$) after surface in Fig. 3 was further annealed at 780 K overnight; (b) $150 \times 150 \text{ \AA}^2$ image ($V_B = -0.3 \text{ V}$, $I_T = 0.6 \text{ nA}$) at the apex of the triangular pyramid indicated.

When the 150-\AA periodic sawtooth ridge structure was further annealed overnight at 740 K, the long-range periodicity was lost but striking arrays of triangular shapes formed all over the surface (Fig. 3). Interconnected and near-perfect mesoscopic isosceles triangles dominate the image, and the $[1\bar{2}1]$ and $[\bar{1}21]$ edges of different layers tend to align themselves forming regions of regular stepped planes. For some of the smaller triangles comprising 10, 15, or 21 atoms (3, 4, or 5 rows, respectively), inverted triangles of missing atoms (triangular troughs) reflected in the $\{120\}$ plane are observed, joined along their $[001]$ edge giving a shadow effect. This resembles the etching patterns formed in the $\text{Cu}(210)\text{-Br}$ system.¹² Large facet planes are fully formed when this surface was again annealed overnight, this time at 780 K (Fig. 4). Figure 4(a) shows well-formed triangular pyramidal facet structures hundreds of angstroms wide at the base. A close-up view of the top of these pyramids in Fig. 4(b) shows they comprise stacked triangular (210) layers, with the triangles increasing in size towards the base. Each side of the pyramid is a fairly regular stepped plane, with $\{210\}$ terraces approximately 4 atoms wide. The stepped planes can be approximately designated $(S)\text{-}[4(210) \times (abc)]$, where (abc) is the respective monatomic step edge plane comprising the low-index $\{100\}$ and $\{110\}$ planes.

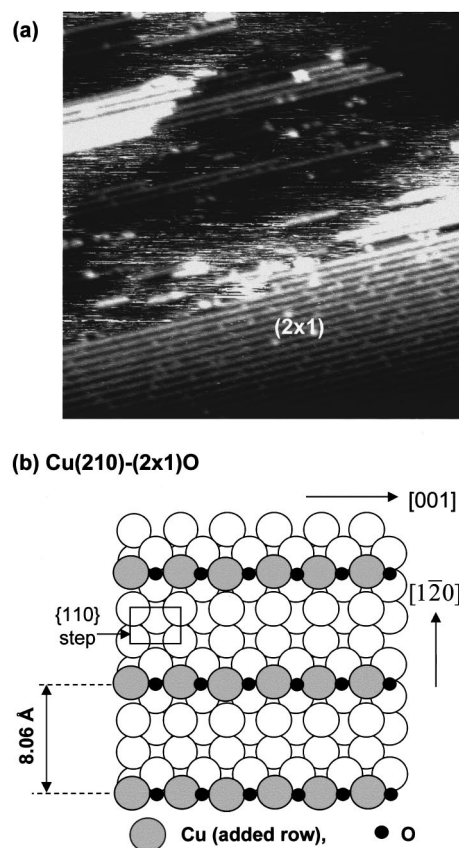


FIG. 5. (a) $300 \times 300 \text{ \AA}^2$ image after exposing clean $\text{Cu}(210)$ at 550 K to 1.0 L oxygen ($V_B = -2.0 \text{ V}$, $I_T = 1.0 \text{ nA}$). (b) Schematic model of the $\text{Cu}(210)\text{-(2 \times 1)O}$ reconstruction.

The above superstructure and faceting behavior is surprisingly quenched when oxygen exposure on $\text{Cu}(210)$ takes place at elevated temperatures. Figure 5 shows that a $\text{Cu}(210)\text{-(2 \times 1)O}$ phase forms after exposure to 1.0 L oxygen at 550 K. The resemblance of the Cu-O rows to those in the $\text{Cu}(110)\text{-(2 \times 1)O}$ system at RT is remarkable. The Cu-O rows also run along the $[001]$ direction, but with a larger inter-row spacing of 8.06 \AA [Fig. 5(b)]. Isolated Cu-O rows nucleate and lengthen via the trapping of mobile Cu and O atoms at the ends of the rows, and eventually cluster to form islands with the (2×1) reconstruction. This is consistent with the observed (2×1) LEED pattern. We found that the (2×1) phase was extremely stable to faceting and remained stable even after annealing to 760 K. Prolonged annealing above 780 K resulted in the depletion of Cu-O rows, but no faceting. Similar behaviour was observed after all oxygen exposures in the temperature range 520–740 K.

It is known that open and rough surfaces restructure more readily upon chemisorption.¹³ However, the unique property of $\text{Cu}(210)$ is its ability to form two distinct and unusual surface reconstructions depending on whether oxygen adsorption occurs at room temperature or above 500 K. There must therefore be an irreversible temperature-dependent process in oxygen adsorption and/or Cu adatom diffusion resulting in either the “grating” superstructure or (2×1) reconstruction, but not both. At RT, oxygen does not inhibit Cu adatom removal from terrace troughs which results in a very irregular surface with numerous multiple step edges. These step edges are believed to be stabilized by oxygen and even-

tually form the stripe edges of the grating superstructure upon brief anneal to 500–600 K. During oxygen exposure above 500 K, however, Cu-O rows preferentially form and this eventually leads to the stable (2×1) phase. Cu adatom removal from terrace troughs is suppressed and step walls are quickly stabilized by the (2×1) phase. In their low-temperature STM experiments, Briner *et al.*¹⁴ established the existence of a molecular oxygen precursor, and concluded that molecular mobility and trapping strongly influence the adsorbate distribution in the O_2 -Cu(110) system, while atomic mobility is of secondary importance. We therefore postulate that the temperature-dependence of oxygen molecular mobility and trapping is a major factor which determines whether stable Cu-O rows or troughs form in the O_2 -Cu(210) system.

Rough surfaces that are chemically active appear to exhibit high adatom mobility and coordinatively unsaturated surface atoms move easily toward new and more bulklike equilibrium positions.¹⁵ Adsorbate-induced restructuring can occur on longer time scales (hours) involving massive restructuring of the surface by atom transport. Restructuring occurs in order to maximize the bonding and stability of the adsorbate-substrate complex. It is driven by thermodynamic forces and occurs when stronger adsorbate-substrate bonds that form compensate for the weakening of bonds between the substrate atoms, an inevitable accompaniment to the chemisorption-induced restructuring process. The Cu(210)-O system is an elegant example of the faceting process. Room temperature adsorption of oxygen followed by brief annealing to 500–600 K results in superstructure formation. Further annealing from about 640 to 780 K for longer duration results in the progressive transformation of this [001]-aligned superstructure to the triangular pyramidal facet structures, with the basic triangular unit reflecting $\{210\}$ symmetry. The

facets probably possess the basic geometry of bulk Cu_2O but further structural studies are required to establish this possibility.

In postulating the structure of Cu(210)- $(2 \times 1)O$, we note that adsorption of O at the long bridge sites of alternate $\{110\}$ steps would facilitate the formation of Cu-O rows such that each O atom maintains a four-coordinate status [Fig. 5(b)]. Using an average Cu-O bond length of 1.91 Å for the Cu(110)- $(2 \times 1)O$ system,² it is possible to estimate the positions of the Cu and O atoms in the added rows assuming no surface relaxation of the substrate Cu atoms. By geometry, the vertical separation of the first and second Cu layers (added rows and top substrate layer) $d_{12} = 1.56$ Å and that between the O layer and second Cu layer $d_0 = 0.94$ Å. Taking into account inevitable surface relaxation effects, the Cu-O rows comprise approximately collinear Cu and O atoms about 1 Å above the next Cu layer. Quantitative LEED experiments will be performed to determine more accurate structural parameters.

In summary, we have used STM to study the chemisorption of oxygen on Cu(210) at RT and elevated temperatures. At RT, oxygen adsorption promotes the formation of terrace troughs, islands and multiple step edges. Annealing to 500–600 K results in a supergrating along the [001] direction with a 30-Å period. Further annealing from 640 to 780 K results in substantial atomic restructuring to form triangular pyramidal facets, with interesting intermediate structures reflecting the $\{210\}$ symmetry. In contrast, oxygen exposure on Cu(210) above 500 K results in a (2×1) reconstruction comprising Cu-O rows along the [001] direction. Faceting of the (2×1) phase was not observed even after large oxygen exposures and subsequent annealing to high temperatures, indicating the stability of this phase. An added row structure for Cu(210)- $(2 \times 1)O$ is also proposed.

*Author to whom correspondence should be addressed. FAX: +65 777 6126. Electronic address: phyweets@nus.edu.sg

¹See, for example, F. Besenbacher, and J. K. Nørskov, *Prog. Surf. Sci.* **44**, 5 (1993), and references therein.

²W. Liu, K. C. Wong, H. C. Zeng, and K. A. R. Mitchell, *Prog. Surf. Sci.* **50**, 247 (1995).

³Y. Kuk, F. M. Chua, P. J. Silverman, and J. A. Meyer, *Phys. Rev. B* **41**, 12 393 (1990).

⁴D. J. Coulman, J. Winterlin, R. J. Behm, and G. Ertl, *Phys. Rev. Lett.* **64**, 1761 (1990).

⁵F. Jensen, F. Besenbacher, E. Laesgaard, and I. Stensgaard, *Phys. Rev. B* **41**, 10 233 (1990).

⁶P. J. Knight, S. M. Driver, and D. P. Woodruff, *Surf. Sci.* **376**, 374 (1997).

⁷C. S. McKee, L. V. Renny, and M. W. Roberts, *Surf. Sci.* **75**, 92 (1978).

⁸F. H. Jones, K. Rawlings, J. S. Foord, P. A. Cox, R. G. Egdell, J. B. Pethica, B. M. R. Wanklyn, S. C. Parker, and P. M. Oliver, *Surf. Sci.* **359**, 107 (1996).

⁹J. Winterlin, R. Schuster, D. J. Coulman, G. Ertl, and R. J. Behm, *J. Vac. Sci. Technol. B* **9**, 902 (1991).

¹⁰A. T. S. Wee, T. W. Fishlock, R. A. Dixon, J. S. Foord, R. G. Egdell, and J. B. Pethica (unpublished).

¹¹K. Kern, H. Niehus, A. Schatz, P. Zeppenfeld, J. Goerge, and G. Comsa, *Phys. Rev. Lett.* **67**, 855 (1991).

¹²A. T. S. Wee, T. W. Fishlock, R. A. Dixon, J. S. Foord, R. G. Egdell, and J. B. Pethica (unpublished).

¹³G. A. Somorjai, *Introduction to Surface Chemistry and Catalysis* (Wiley, New York, 1994), p. 56 ff., and references therein.

¹⁴B. G. Briner, M. Doering, H.-P. Rust, and A. M. Bradshaw, *Phys. Rev. Lett.* **78**, 1516 (1997).

¹⁵G. A. Somorjai, *Introduction to Surface Chemistry and Catalysis* (Ref. 13), p. 412 ff.